

INVESTIGATION OF PALU TUNNEL DEFORMATIONS ALONG THE CREEPING SECTION (HAZAR-PALU SEGMENT) OF THE EAST ANATOLIAN FAULT, TURKEY BY TERRESTRIAL LASER SCANNER

Ugur Dogan (1), Bulent Bayram (1), Semih Ergintav (2), Alper Yigitoglu (1),
Ziyadin Cakir (3), Cengiz Zabcı (3), Hayrullah Karabulut (2)

1 Yildiz Technical University, Department of Geomatics Engineering, Davutpasa
Campus, Esenler, 34220, Istanbul-Turkey

2 Bogazici University, Kandilli Observatory and Earthquake Research Institute
Department of Geodesy, Cengelkoy, 34680, Istanbul-Turkey

3Istanbul Technical University, Faculty of Mines, Department of Geology, Maslak,
34469, Istanbul-Turkey

Email: dogan@yildiz.edu.tr; bayram@yildiz.edu.tr; semih.ergintav@boun.edu.tr;
motifharita@hotmail.com; ziyadin.cakir@itu.edu.tr; zabcı@itu.edu.tr;
kara@boun.edu.tr

KEY WORDS: Terrestrial Laser Scanner, surficial deformation, change detection, photogrammetry

ABSTRACT: The Eastern Anatolian Fault (EAF), which forms the boundary between Anatolia and Arabian plates, is one of the most important tectonic structures in the Eastern Mediterranean region. Together with its conjugate, the North Anatolian Fault (NAF), it accommodates the westward motion of the Anatolian plate with respect to Eurasia. Although it has been associated only with small-to-moderate sized earthquakes in the instrumental period and relatively quiet compared to the North Anatolian Fault, the EAF produced devastating large ($M > 7$) earthquakes in the historical time. Analysis of historical seismicity suggests that a seismic gap exists between the Lake of Hazar and Bingöl, referred here as to Palu seismic gap. Recently, using GPS and InSAR, we showed that the 100km-long section of the Palu segment is exhibiting aseismic creep at the surface, in contrast to the previous studies. The creep rate varies along the fault reaching, at some places, to the far field GPS-based plate velocity (i.e., 10 ± 0.3 mm/yr), implying that significant portion of the elastic strain has been released aseismically. One of the best markers of the creeping zone is Palu railway tunnel that is 4.90m wide, 5.87m high and 787m long. It cuts by EAF and the walls of the tunnel have been offset by approximately 10-20 cm since construction in the middle of the last century.

In this study, surface deformation of the tunnel has been investigated using Terrestrial Laser Scanner (TLS). The measurements have been performed using FARO Focus 3D X130 on 10.09.2018 and 19.06.2019, respectively. The first TLS data has been taken as reference for registration of the second TLS measurement. The registration accuracy has been calculated as 3.02 mm. Open source Cloud Compare software has been used to define changes between two- dataset. 2.05% of calculated distances were in 1 - 2.5 cm interval. However, in some small regions, distances varying between 2.5-5 cm have been observed. In this study, effects of calculated distances on the stabilization of the structure are discussed. This study showed that the TLS technique gives promising results for monitoring of surface deformation of Palu railway tunnel.

1. INTRODUCTION

The fundamental knowledge of the dynamics of the Earth's crust is today limited by a clear understanding of the links between seismic behavior and slow deformations along active faults (Beroza ve Ide, 2011). Silent slow slip events, tremors, repeating earthquakes, posts-seismic slip and aseismic creep; all these recent discoveries shed new light on the dynamics of the Earth's crust at the global scale and on the seismic cycles (Peng ve Gomberg, 2010; Barbot vd., 2012). The existence of physical and geological links between all these observations is strongly suggested by recent observations which show that many large earthquakes are preceded by a long nucleation phase (Bouchon vd., 2011, 2013) involving creep or that, conversely, fault creep often initiates after earthquake rupture (e.g. Izmit 1999 earthquake afterslip; Çakır et al., 2012). Because creep processes transfer stress between different portions of the fault, by relaxing or loading them, they control the nucleation of large earthquakes. These discoveries of active aseismic deformations provide a paradigm shift on how tectonic forces are dissipated along faults zones and how large earthquakes may nucleate.

With the recent seismic activity on the East Anatolian Fault (EAF), which forms the boundary between Anatolia and Arabian plates, it has been concluded that it is highly likely that there is a significant creep behavior on the upper crust on the EAF, as in the North Anatolian Fault (NAF) (Fig. 1). Analysis of historical seismicity suggests that a seismic gap exists between the Lake of Hazar and Bingöl, referred here as to Palu seismic gap.

Nalbant et al. (2002) analyzed the seismic hazard in the region using 11 earthquakes of magnitude $M \geq 6.7$ on the EAF from 1822 to the present. The results showed that there was a seismic gap between Palu and Hazar Lake and will be the probability of an earthquake of 7 or more in the region. Also, different researchers have supported this finding that the region will produce an earthquake of magnitude $M > 7.4$ using geology, paleoseismology, historical earthquake activity, and GPS data. (Çetin et al., 2003; Duman and Emre, 2013, Aktug et al., 2016).

TLS is an efficient technique for rapid 3D point cloud acquisition and surface deformation analysis (Xu, et al., 2018). Tunnel deformation monitoring has vital importance for engineers. Tape extensometer (Kolymbas, 2005), Bassett Convergence System (Bassett et al., 1999), total station (Mukupa, et al., 2016) are traditional deformation surveying methods. TLS is a new technique for detection of tunnel deformation (Cui, et al., 2019) which overcomes the limitations of conventional techniques (Xie and Lu, 2017).

The quality of the TLS point cloud data depends on different factors as structure of tunnel surface, environmental conditions and type of instrument (Wang, et al., 2014). TLS measurements and deformation analysis topic have been studied by many researchers in the literature. Lam (2006) investigated the efficiency of TLS for tunnel deformation. Cabo, et al., (2017) proposed a new method to find optimal TLS positions for measurements in tunnels. Fekete et al., (2010) used triangular mesh for detection of underbreak and overbreak zones in tunnels. Xie and Lu, (2017) proposed a 3D modelling algorithm for monitoring of tunnel deformation. Yang, et al., (2018) proposed an automatic B-spline model for optimizing composite tunnel model by analyzing over- and under-fitting problems of different point cloud profiles. Cheng, et al., (2019) integrated TLS data to building information model (BIM) for a single-track railway tunnel. Yi, et al., (2019) proposed a hierarchical approach for tunnel modelling from raw TLS data. Xu, et al., (2019) proposed a near real-time method for quality inspection of tunnels using point cloud data.

Since Palu railway tunnel is on the EAF, in addition to the geodetic measurements, monitoring of surface deformation is essential for monitoring of structural changes of the tunnel. Therefore, in this study, surface deformation of the Palu tunnel has been investigated using multiple TLS dataset. Open source CloudCompare software has been used for point cloud based change detection. Our results showed that the tools of the used software and TLS technique give promising results for temporal change detection analysis and monitoring for tunnels.

2. STUDY AREA

In a recent study, , we showed that the 100km-long section of the Palu segment is exhibiting aseismic creep at the surface using GPS and InSAR, in contrast to the previous studies. The creep rate varies along the fault reaching, at some places, to the far field GPS-based plate velocity (i.e., 10 ± 0.3 mm/yr), implying that significant portion of the elastic strain has been released aseismically (Ergintav et al., 2018).

Tectonic map of the study area is given in Figure 1. The bold black lines indicate the two major faults of Turkey; the NAF and the EAF. The lower right corner of the map shows the active fault map of Turkey (Emre et al., 2013) and its vicinity with GPS velocity rates with respect to Eurasia (Reilinger et al., 2006).

One of the best markers of the creeping zone is Palu railway tunnel that is 4.90 m wide, 5.87 m high and 787 m long. It is cut by EAF and the walls of the tunnel have been offset by approximately 10-20 cm since construction in the middle of the last century (Figure 2).

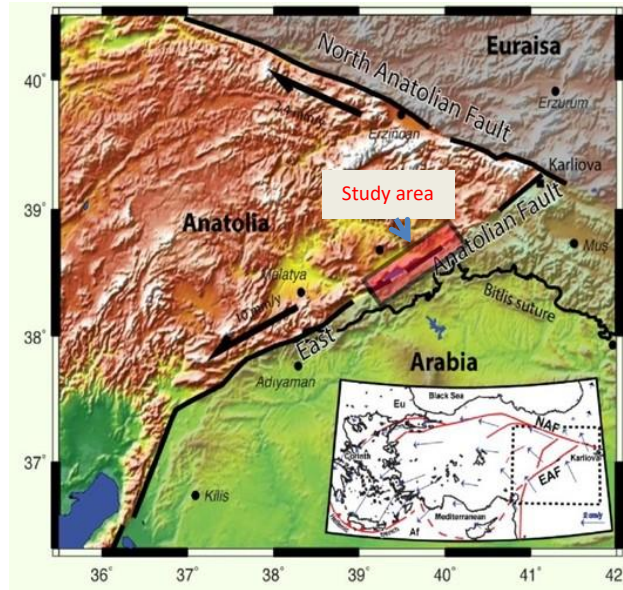


Figure 1 Study area

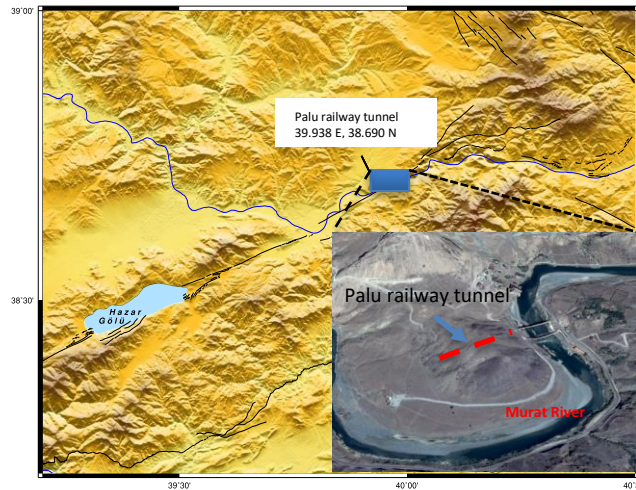


Figure 2 Palu railway tunnel

3. MATERIALS AND METHODS

This study consists of three main steps namely as: (i) registration of 20 sub-scanning on 9 October 2018 (first measurement), (ii) registration of 16 sub-scanning on 19 June 2019 (second measurement) and (iii) comparison of two point cloud data for deformation investigation.

Faro Focus 3D x130 was used for scanning of the tunnel. Scanning time at each station was approximately 3 minutes. The scanning density was set as 6 mm for 10 m scanning distance which corresponds to 43 million point cloud per scan. Each sequential scan was performed with approximately 80% overlap. Due to poor illumination conditions in the tunnel, the scans were done without colour capture and the point cloud have been obtained in greyscale. TLS measurements in the Palu railway tunnel were carried out in a corridor of 100 m including 50 m left and right sides of fault. The analyses were realized considering 75 m part of the tunnel. During the laser scanning, black and white target is fixed to the so-called Escape chambers in the tunnel (Figure 3).



Figure 3 Control points in the tunnel

TLS measurements for first dataset have been performed in 5 m intervals in the tunnel (Figure 4) and registration processes of 20 stations have been carried out using cloud to cloud technique. 1 natural, 8 paper targets and 17 sphere targets have been used as check points.

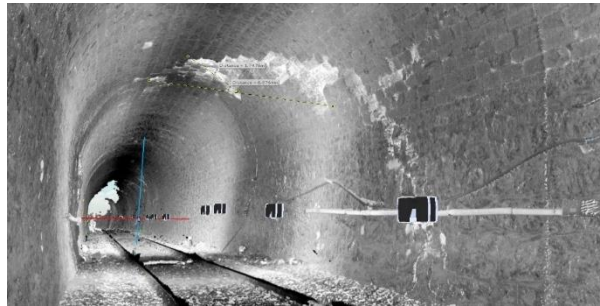


Figure 4 TLS scanning in the tunnel

Target-less registration has two steps that are coarse registration and fine registration. First, matching correspondences are found between overlapping scans and then least squares adjustment is utilized iteratively (Abbas, et al, 2014). Iterative Closest Point (Besl and McKay, 1992), Plane-based matching algorithms (Bellekens, et al., 2014), three dimensional surface matching using 3D boxing (Akca and Gruen, 2007) can be given as some coarse registration methods. The used FARO scene software uses a plane-based matching algorithm for coarse registration.

The paper targets that were used in the first scan were not moved and they have been also used for registration of the second TLS measurements. 1 natural, 8 paper targets and 20 spheres target have been used as check points for the second dataset. The scanning time for each station was approximately 3 minutes.

Point cloud comparison has been performed using distance computation module of the open source software (Cloud Compare, 2019). Cloud-to-cloud comparison is realized with the closest point technique based on octree structure (Bakirman, et al., 2017). For each point of the target point cloud, the closest point is defined in the reference point cloud (Lague, et al., 2013). This method is based on the main idea that is “reference cloud is dense enough, then the nearest neighbor distance will be (almost) as accurate as the true distance” (Girardeau-Montaut, 2015).

4. RESULTS AND DISCUSSION

In this study, preliminary surface deformation results of Palu railway tunnel have been obtained within the scope of “Multi-disciplinary studies on the characteristics of surface creep along the Hazar-Palu Segment of the East Anatolian Fault” project for one year period. First, all TLS data have been registered using the cloud to cloud technique. For the first scan (10.09.2018, with 20 scan stations), the average registration error was calculated as 1.96 mm. Minimum and maximum errors were 1.24 mm and 2.95 mm, respectively. For the second scan (10.09.2018, with 16 scan stations), the average registration error was calculated as 2.94 mm. Minimum and maximum errors were 4.79 mm and 1.15 mm, respectively. The registered point clouds and generated mesh models for both dataset have been given in Figure 5(a),(b),and Figure 5(c), (d), respectively.

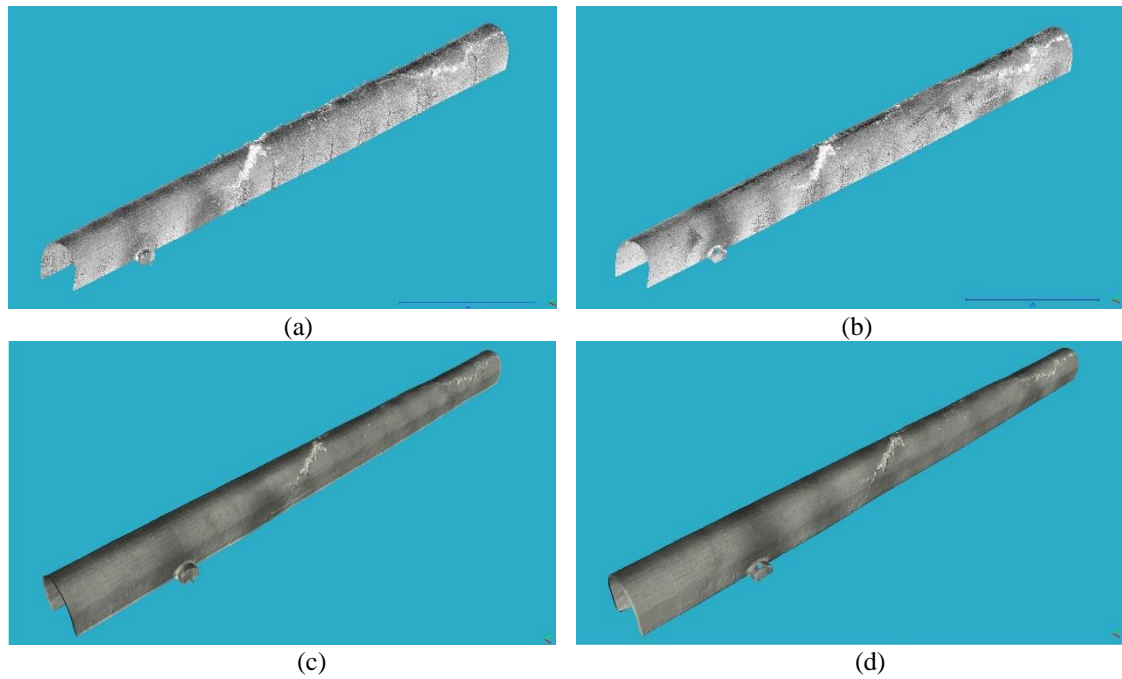


Figure 5 registered point cloud of Palu railway tunnel

To detect temporal changes in the tunnel, the first registered point cloud has been taken as reference and the second one is registered using targets in the tunnel (Figure 6). A total of two natural points and six targets have been used for this purpose. The average registration error has been calculated as 4.7 mm.

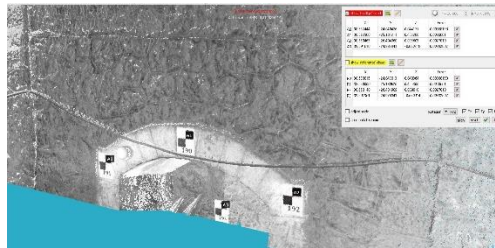


Figure 6 Used targets for registration

Two registered point cloud data have been compared using open source Cloud Compare software. The calculated differences between 0 - 5 cm are given in Figure 7.

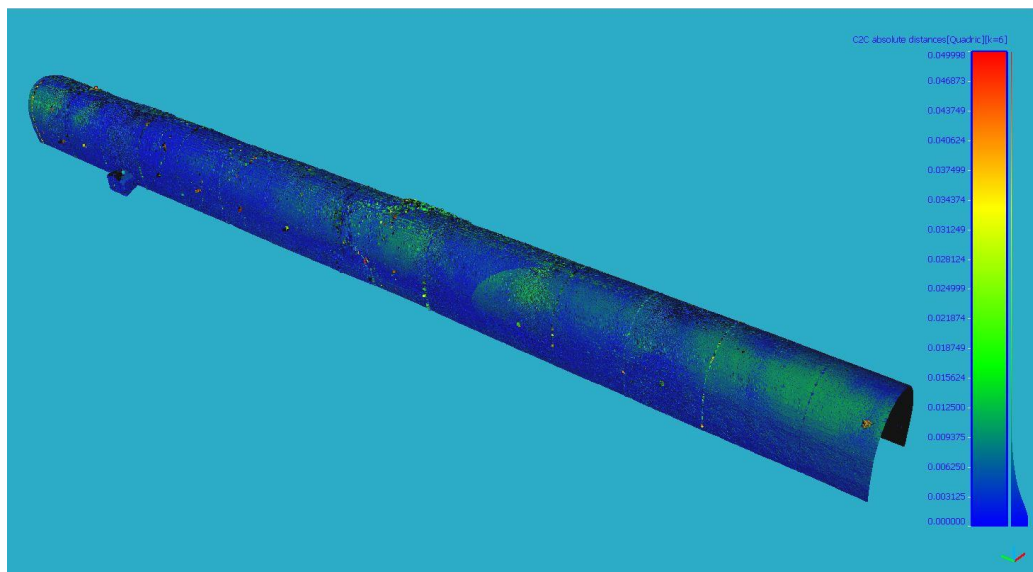
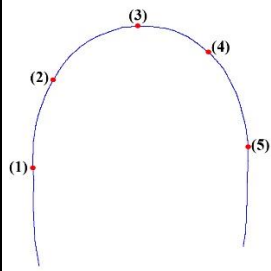


Figure 7 Calculated distances between two point cloud data

80.55%, 17.24%, 2.05% and 0.15% from 33,136,605 points fall within the intervals of 0 -0.5 cm, 0.55 - 1cm, 1 - 2.5 cm and 2.5 - 5 cm, respectively. As can be seen in Figure 6, the highest distances have been calculated on the top heading and mostly on the right side of the fault cut point of the tunnel. It has been thought that, the activities of fault affected this part of the tunnel. In additionally, the differences have been measured in eight cross-sections in 10 m space length. Differences between two point clouds approximately at 5 points in each section were measured and the results have been given in Table 1.

Table 1 Cross-section measurements

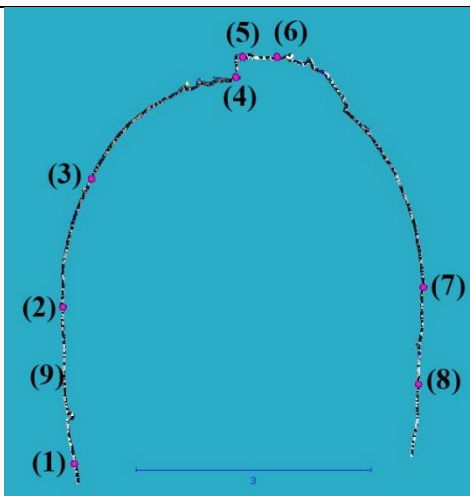
Cross-section measurements								
		1	2	3	4	5	6	7
Point no/ differences (mm)	1	3.6	4.13	2.5	4.72	8.77	7.51	3.73
	2	5.7	6.91	5.85	8.1	5.2	6.32	9.4
	3	6.01	7.22	10.57	19.66	12.63	9.69	13.52
	4	2.12	6.15	6.99	7.15	3.64	6.54	11.47
	5	5.36	5.06	5.04	2.22	6.47	1.43	7.54
min		2.12	4.13	2.50	2.22	3.64	1.43	3.73
max		6.01	7.22	10.57	19.66	12.63	9.69	13.52
average		4.32	5.96	7.13	10.18	7.80	5.76	9.96



One cross-section was taken from the point where the fault cut the tunnel. Differences have been calculated at 8 points. The results are given in Table 2.

Table 2 Cross-section where the fault cut the tunnel

Cross-section measurement		
		8
Point no/ differences (mm)	1	5.8
	2	10.15
	3	7.59
	4	238.62
	5	45.24
	6	13.81
	7	7.3
	8	6.78
min		5.80
max		238.62
average		41.91



The local deformations have been observed at the fault-cut cross-section. 24 cm of the collapse was calculated at point 5 (Figure 8). Obtained surface comparison results depict that there are activities in Palu railway tunnel and it has to be taken into consideration.



Figure 8 Fault zone in the Palu railway tunnel

Another result of the study is the efficiency of TLS technique for temporal tunnel monitoring. The surface change zones in the tunnel have been determined efficiently. However, these results should be monitored and verified with further measurements. We plan to conduct a new TLS measurements to further investigate temporal changes in the tunnel. Thus, we will have a great opportunity to verify the deformations with of the mounted creep meter measurements (Figure 8) in micrometer unit.

5. CONCLUSIONS

In this study, TLS data were applied to surface deformation monitoring of Palu railway tunnel. TLS measurements have been done two times in one year and period point cloud data have been compared using with the proposed framework using open source CloudCompare software. The distances between two point cloud data have been calculated based on nearest neighbor method. It has been seen that TLS technique is efficient and flexible for surface deformation monitoring. The Palu railway tunnel is cut directly by the fault zone and its deepest surface is approximately 50 m. The achieved surface deformation zones will play key role to determine the effect of fault zone to the tunnel. Additionally, the deformations will be observed regarding to TLS measurements. Two Creepmeter stations were also mounted in the tunnel for effective measurement of tunnel deformations with high sensitivity (micron size). Changes in a stretched wire over the observed region are measured digitally in both stations. After the next period of measurements, it will be possible to verify both TLS and creepmeter results.

As a future project, we are firstly planning to employ structure from motion photogrammetry to obtain point cloud data from images. We are about to develop a tunnel photographing system with special construction. Thus, TLS data will be integrated with image derived point cloud including detailed texture information. As the railway is actively used, the working times are limited. Therefore, an optimizing for measurements and scanning stations is essential. This issue will be our second project aiming to realize TLS measurements in short time. Finally, we will develop an automated point cloud segmentation method to utilize non-parametric and accurate deformation investigations using texture information.

Acknowledgments

This paper summarized the preliminary he results of experiments performed to verify measurement precision (supported by TUBITAK 1001 projects 114Y250 and 118Y450).

References

- Abbas, M A, Luh., L C, Setan, H, Majid, Z, Chong, A K, Aspuri, A, Idris, K M, Ariff, M F M .2014. Terrestrial laser scanners pre-processing: registration and georeferencing. *Jurnal Teknologi*, 71 (4). pp. 115-122. ISSN 0127-9696.
- Akca, D. and Gruen A. 2007. Generalized least squares multiple 3d surface matching, *IAPRS Volume XXXVI, Part 3 / W52*, pp. 1-7.
- Aktug, B., Nocquet, J. M., Cingoz, A., Parsons, B., Ercan, Y., England, P. C., Lenk, O., Gurdal, M., Kilicoglu, A., Akdeniz H., Tekgul, A. 2010. Deformation of western Turkey from a combination of permanent and campaign GPS data: limits to block-like behavior, *Journal of Geophysical Research*, 114, B10404.
- Bakirman T., Gumusay M. U., Catal Reis H., Selbesoglu M. O., Yosmaoglu S., Yaras M. C., Seker D. Z., And t Bayram B. 2017, Comparison of low cost 3D structured light scanners for face modelling, *Applied Optics*, Vol. 56, No. 4 / February 1 2017 / , p.985-992.
- Barbot, S., Lapusta, N., and Avouac, J.P., 2012. Under the hood of the earthquake machine: Toward predictive modeling of the seismic cycle: *Science*, v. 336, no. 6082, p. 707–710, doi: 10.1126/science.1218796.
- Bassett, R., Kimmance, J., Rasmussen, C., 1999. An automated electrolevel deformation monitoring system for tunnels. *Proceedings of the Institution of Civil Engineers-Geotechnical engineering* 137, 117-125.
- Bellekens, B, Spruyt, V, Berkvens, R, and Weyn, M. 2014. A Survey of Rigid 3D Pointcloud Registration Algorithms”, *AMBIENT 2014: The Fourth International Conference on Ambient Computing, Applications, Services and Technologies*, pp. 8-13.

- Besl P.J., McKay N.D., A method for registration of 3D shapes, *IEEE Transactions on Pattern Analysis and Machine Intelligence* 14 (1992) 239–254.
- Beroza, G. C., & Ide, S. 2011. Slow earthquakes and nonvolcanic tremor. *Annual review of Earth and planetary sciences*, 39, 271-296.
- Cabo C., Ordóñez C., Argüelles-Fraga R. 2017. An algorithm for optimizing terrestrial laser scanning in tunnels, *Automation in Construction*, 83,163–168.
- Çakir, Z., Ergintav, S., Özener, H., Dogan, U., Akoglu, A. M., Meghraoui, M., & Reilinger, R. 2012. Onset of aseismic creep on major strike-slip faults. *Geology*, 40(12), 1115-1118.
- Çetin, H., Guneyli, H., Mayer, L. 2003. Paleoseismology of the Palu-Lake Hazar segment of the East Anatolian fault in Turkey, *Tectonophysics*, 374, 163-197.
- Cheng Y., Qiu W., Duana D. 2019. Automatic creation of as-is building information model from single-track railway tunnel point clouds, *Automation in Construction*, 106 ,102911, <https://doi.org/10.1016/j.autcon.2019.102911>.
- Cloud Compare, 2019, Retrieved on 30 August 2019 from http://www.danielgm.net/cc/doc/qCC/Documentation_CloudCompare_version_2_1_eng.pdf .
- Cui H., Ren X., Mao Q., Hu Q., Wang W. 2019. Shield subway tunnel deformation detection based on mobile laser scanning, *Automation in Construction*, 106 , 102889, <https://doi.org/10.1016/j.autcon.2019.102889>.
- Duman, T., Emre, O., 2013. The East Anatolian Fault; geometry, segmentation and jog characteristics(inGeological development of Anatolia and the easternmost Mediterranean region), *Special Publication - Geological Society of London*, 372(1), 495-529.
- Emre, O., Duman, T. Y., Ozalp, S., Elmaci, H., Olgun, S., Saroglu, F. 2013. Active fault map of Turkey with and explanatory text. General Directorate of Mineral Research and Exploration, Special Publication Series-30, Ankara, Turkey.
- Ergintav, S., Çetin, S., Şentürk, S., Özdemir, A., Çakır, Z., Doğan, U., Karabulut, H., Şaroğlu, F., Dikmen, Ü., Bilham, Julaiti R.W., Özener, H., 2018. New evidence for spatiotemporal fluctuations of slip rate on the East Anatolian Fault, Turkey from newly installed creepmeters and seismological data, *European Geosciences Union General Assembly, Geophysical Research Abstracts*, Vol. 20, 9395, 08-13 April, Vienna, Austria.
- Fekete, S., Diederichs, M., Lato, M. 2010. Geotechnical and operational applications for 3-dimensional laser scanning in drill and blast tunnels. *Tunnelling and Underground Space Technology* 25, 614-628.
- Girardeau-Montaut D., 2015. CloudCompare CICESE Workshop, Retrieved on 26 August 2019 from https://cloud.sdsc.edu/v1/AUTH_opentopography/www/shortcourses/15_NPAC/CloudCompare_workshop_CICESE.pdf.
- Kolymbas, D., 2005. *Tunnelling and tunnel mechanics-A rational approach to tunnelling*. Springer. Lemmens, M., 2011. *Geo-information*. Springer, [s.l.].
- Lague D., Brodu N., Leroux J. 2013. Accurate 3D comparison of complex topography with terrestrial laser scanner: Application to the Rangitikei canyon (N-Z), *ISPRS Journal of Photogrammetry and Remote Sensing*, Volume 82, August 2013, Pages 10-26, <https://doi.org/10.1016/j.isprsjprs.2013.04.009>.
- Lam S.Y.W. 2006. Application of terrestrial laser scanning methodology in geometric tolerances analysis of tunnel structures, *Tunn. Undergr. Space Technol.* 21 (2006), <http://dx.doi.org/10.1016/j.tust.2005.12.057>.
- Lague D., Brodu N., Leroux J. 2013. Accurate 3D comparison of complex topography with terrestrial laser scanner: Application to the Rangitikei canyon (N-Z), *ISPRS Journal of Photogrammetry and Remote Sensing*, Volume 82, August 2013, Pages 10-26, <https://doi.org/10.1016/j.isprsjprs.2013.04.009>.
- Mukupa W., Roberts G.W., Hancock C.M., Manasir K. Al-, 2016. A review of the use of terrestrial laser scanning application for change detection and deformation monitoring of structures, *Empire Surv. Rev.* 49 (353) (2016) 99–

116, <https://doi.org/10.1080/00396265.2015.1133039>.

Nalbant, S., McCloskey, J., Steacy, S. and Barka, A. 2002. Stress accumulation and increased seismic risk in eastern Turkey, *Earth and Planetary Science Letters*, 195, 291-298.

Peng, Z., & Gomberg, J. 2010. An integrated perspective of the continuum between earthquakes and slow-slip phenomena. *Nature Geoscience*, 3(9), 599-607.

Reilinger, R., McClusky, S., Vernant, P., Lawrence, S., Ergintav, S., Cakmak, R. Özener, H., Kadirov, F., Guliev, I., Stepanyan, R., Nadariya, M., Habubia, G., Mahmoud, S., Sakr, K., ArRajehi, A., Paradissis, D., Al-Aydrus, A., Prilepin, M., Guseva, T., Evren, E., Dmitritsa, A., Filikov, S. V., Gomez, F., Al-Ghazzi, R., & Karam, G. 2006. GPS constraints on continental deformation in the Africa-Arabia-Eurasia continental collision zone and implications for the dynamics of plate interactions. *Journal of Geophysical Research: Solid Earth (1978–2012)*, 111(B5).

Wang W., Zhao W., Huang L., Vimarlund V., Wang Z. 2014. Applications of terrestrial laser scanning for tunnels: a review, *Journal of Traffic and Transportation Engineering (English Edition)* Volume 1, Issue 5, October 2014, Pages 325-337, [https://doi.org/10.1016/S2095-7564\(15\)30279-8](https://doi.org/10.1016/S2095-7564(15)30279-8).

Xie X. and Lu X., 2017. Development of a 3D Modeling Algorithm for Tunnel Deformation Monitoring Based on Terrestrial Laser Scanning, *Underground Space*, Volume 2, Issue 1, March 2017, Pages 16-29.

Xu J. Ding L., Luo H., Chen E., Wei L. 2019. Near real-time circular tunnel shield segment assembly quality inspection using point cloud data: A case study, *Tunneling and Underground Space Technology*, 91, 102998, <https://doi.org/10.1016/j.tust.2019.102998>.

Xu X., Yanga H., Neumann I. 2018. Deformation monitoring of typical composite structures based on terrestrial laser scanning technology, *Composite Structures*, 202, 77–81.

Yang, H., Xu, X., Kargoll, B., Neumann, I. 2018. An Automatic and Intelligent Optimal Surface Modeling Method for Composite Tunnel Structures, *Composite Structures*, Volume 208, 15 January 2019, Pages 702-710, doi: <https://doi.org/10.1016/j.compstruct.2018.09.082>.

Yen, K S, Akin, K, Ravani, B, Lasky T A. 2013. Accelerated Project Delivery: Case Studies and Field Use of 3D Terrestrial Laser Scanning in Caltrans Projects: Phase II- Additional Training and Materials, AHMCT Research Center, California Department of Transportation, Sacramento. Report Number, CA08-1697, AHMTC Research Method, UCD-ARR-08-06-30-06. Retrieved on 23 August 2019, from <http://ahmct.ucdavis.edu/pdf/UCD-ARR-08-06-30-06.pdf>.

Yi, C., Lu, D., Xie, Q., Liu, S., Li, H., Wei, M., & Wang, J. 2019. Hierarchical tunnel modeling from 3D raw LiDAR point cloud. *Computer-Aided Design*, 114,143-154, doi:10.1016/j.cad.2019.05.033.